

# Diffusion Modeling of Percutaneous Absorption Kinetics. 1. Effects of Flow Rate, Receptor Sampling Rate, and Viable Epidermal Resistance for a Constant Donor Concentration

YURI G. ANISSIMOV AND MICHAEL S. ROBERTS\*

Contribution from *Department of Medicine, University of Queensland, Princess Alexandra Hospital, Woolloongabba, Queensland, 4102, Australia.*

Received February 18, 1999. Accepted for publication July 19, 1999.

**Abstract** □ A diffusion model for the percutaneous absorption of a solute through the skin is developed for the specific case of a constant donor concentration with a finite removal rate from the receptor due to either perfusion rate or sampling. The model has been developed to include a viable epidermal resistance and a donor–stratum corneum interfacial resistance. Numerical inversion of the Laplace domain solutions were used for simulations of solute flux and cumulative amount absorbed and to model specific examples of percutaneous absorption. Limits of the Laplace domain solutions were used to define the steady-state flux, lag time, and receptor concentration. Steady-state approximations obtained from the solutions were used to relate the steady-state flux and the effective permeability coefficient to the viable epidermis resistance, a donor–stratum corneum interfacial resistance, receptor removal rate, and partitioning between the receptor and donor phases. The lag time was shown to be dependent on these parameters and on the volume of the receptor phase. It is concluded that curvilinear cumulative amount and flux–time profiles are dependent on the processes affecting percutaneous absorption, the shapes of the profiles reflecting the processes most determining transport.

## Introduction

The interpretation of percutaneous absorption kinetics is highly dependent on the assumed mathematical model representation of transport across the epidermis. This information is then commonly applied to (1) optimize topical formulations, (2) develop transdermal delivery systems, (3) provide risk assessment for skin contaminants, and (4) predict the effect of physiological processes (such as changes in dermal blood flow) on the rate of percutaneous penetration.<sup>1</sup> A number of mathematical models have been used to describe percutaneous absorption kinetics.<sup>2</sup> Most percutaneous absorption kinetic models describe the time dependency of the cumulative amount of solute penetrating the epidermis into a sink receptor phase.<sup>2</sup> The models derived recognize constant and depleting donor concentrations and the resistance of the viable epidermis. When a constant donor concentration exists, the cumulative amount of solute penetrating the epidermis under steady-state conditions ( $Q_{ss}(t)$ ) is linearly related to the exposure time  $t$ :

$$Q_{ss}(t) = J_{ss}A(t - \text{lag}) \quad (1)$$

where  $J_{ss}$  is the steady-state flux, lag is the lag time, and  $A$  is the area of application. The steady-state flux of solutes through the epidermis can be expressed in terms of an apparent permeability coefficient  $k_p$ , and the difference in

vehicle ( $C_{d0}$ ) and receptor compartment ( $C_{r\ ss}$ ) concentrations:<sup>1–4</sup>

$$J_{ss} = k_p(C_{d0} - C_{r\ ss}) \quad (2)$$

A number of studies have shown that  $k_p$  is defined by the resistances of both the stratum corneum and viable epidermis.<sup>4–7</sup>  $C_{r\ ss}$  is defined by  $k_p$ ,  $A$ ,  $C_{d0}$ , and the rate of removal of solute from the receptor compartment, designated as a clearance  $Cl_r$ :<sup>8</sup>

$$C_{r\ ss} = \frac{k_p A C_{d0}}{Cl_r + k_p A} \quad (3)$$

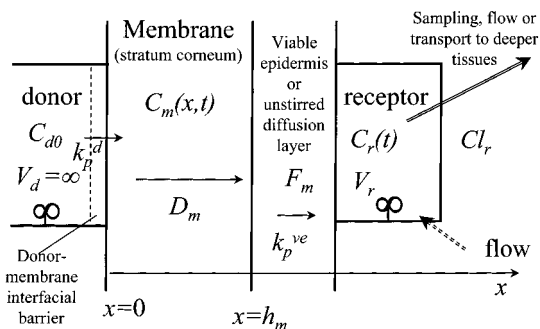
It is apparent that an increased  $Cl_r$  will reduce  $C_{r\ ss}$  (eq 3) and, accordingly, increase  $J_{ss}$  (eq 2). A number of studies have shown that an increase in perfusion flow rate can increase percutaneous absorption.<sup>9–11</sup> In addition, a number of studies have shown that percutaneous absorption of lipophilic solutes is highly dependent on the nature of the receptor fluid and that certain receptor fluids underestimate *in vivo* absorption.<sup>12–19</sup>

We are not aware of mathematical expressions describing the curvilinear  $Q(t)$  versus time profiles associated with nonsink conditions using a diffusion model for epidermal transport. Guy and Hadgraft<sup>20</sup> have given a theoretical expression for the diffusion-controlled release of a solute from a slab into a nonsink receptor. Curvilinear  $Q(t)$  versus time profiles also occur when there is depletion in the donor phase associated with the application of a finite donor.<sup>2</sup> Parry et al.<sup>21</sup> presented an expression for the accumulation of solute in the receptor compartment with time when there was no clearance of solute from the receptor. Guy and Hadgraft<sup>22</sup> reported a pharmacokinetic model in which the influx into the membrane was assumed to be an exponential decline in vehicle concentration and the efflux from the membrane was defined by a first-order rate constant.

In this paper, we derive diffusion equations for the cumulative amount of solute penetrating through the epidermis from a constant donor concentration into a finite receptor volume with a finite removal clearance. Given the potential contribution of the viable epidermis and unstirred water layers as a resistance to transport into the dermis or receptor,<sup>1–7</sup> we have included this effect in our derivations. We have also included the complementary contribution of the vehicle–stratum corneum resistance, as this is relevant to transdermal patch delivery with delivery being controlled in part by a membrane or adhesive patch component. The Laplace expressions for cumulative amount–time and flux–time relationships are then used to define steady-state flux and lag times. These expressions were also used to characterize the effects of changing various determinants on the profiles described by the relationships and to explain experimental data. Given that

\* Corresponding author. Fax: 61-7-3240 5806. E-mail: M.Roberts@mailbox.uq.edu.au.

### A. *In vitro*



### B. *In vivo*

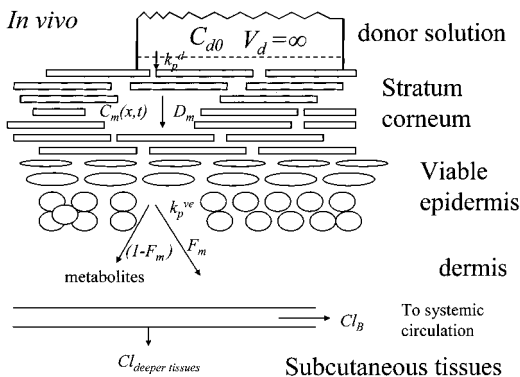


**Figure 1**—Schematic diagram of the model. (A) *In vitro* and (B) *in vivo* (see text for explanations of symbols).

many receptor fluids yield percutaneous absorption fluxes *in vitro* considerably lower than for *in vivo* with highly lipophilic compounds,<sup>23</sup> we have also considered the estimation of the apparent permeability coefficient from the apparent solubility of the solutes in a given receptor fluid.

## Theory

Figure 1 shows a schematic diagram of the model used in this work. Both donor and receptor phases are represented as a well stirred compartments. The transport of solute through the stratum corneum, referred to in this section as the membrane, is described by the diffusion equation:

$$\frac{\partial C_m}{\partial t} = D_m \frac{\partial^2 C_m}{\partial x^2} \quad (4)$$

where  $C_m(x,t)$  is the concentration of solute in the membrane at distance  $x$  at time  $t$ , and  $D_m$  is the diffusion coefficient. We assume there is no solute initially present in the membrane. The initial condition is therefore:

$$C_m(x,0) = 0 \quad (5)$$

The boundary conditions at the donor surface ( $x=0$ ) are defined by the partitioning of the solute between donor phase and membrane:

$$C_m(0,t) = K_m C_{d0} \quad (6)$$

where  $C_{d0}$  is the concentration in the donor phase,  $K_m$  is the partition coefficient between the membrane and donor ( $K_m = C_m^{ss}/C_d^{ss}$  at the equilibrium between the membrane and donor).

**Donor Surface Boundary Conditions**—When an interfacial barrier exists adjacent to the membrane in the

donor phase, boundary condition 6 becomes:

$$-D_m \frac{\partial C_m}{\partial x} \Big|_{x=0} = k_p^d \left( C_{d0} - \frac{C_m}{K_m} \right) \quad (7)$$

where  $k_p^d$  is permeability coefficient through this barrier. In the specific case when this barrier is an unstirred diffusion layer in the donor phase,  $k_p^d = D_{dl}/h_{dl}$ , where  $D_{dl}$  and  $h_{dl}$  are diffusion coefficient and thickness of the layer.

**Receptor Surface Boundary Conditions**—The boundary conditions at the receptor surface ( $x=h_m$ ,  $h_m$  is effective thickness of the membrane) are:

$$-D_m \frac{\partial C_m}{\partial x} \Big|_{x=h_m} = k_p^{ve} \left( \frac{C_m}{K_m} - \frac{C_r}{K_r} \right) \quad (8)$$

$$V_r \frac{dC_r}{dt} = -AD_m \frac{\partial C_m}{\partial x} \Big|_{x=h_m} - Cl_r C_r \quad (9)$$

where  $Cl_r$  is the removal rate (mL/min) of solution containing solute from the receptor phase,  $V_r$  is the volume of the receptor,  $K_r$  is the partition coefficient between the receptor and donor ( $K_r = C_r^{ss}/C_d^{ss}$  at the equilibrium between the receptor and donor),  $A$  is the area of application, and  $C_r$  is the concentration in the receptor. In eq 8,  $k_p^{ve}$  is the permeability coefficient of solute due to a barrier between the membrane and receptor. In the specific case of the viable epidermis or an unstirred aqueous diffusion layer being the barrier,  $k_p^{ve} = K_{ve} D_{ve}/h_{ve}$  where  $h_{ve}$  is the thickness of the viable epidermis/layer,  $D_{ve}$  is the diffusion coefficient in the viable epidermis/layer, and  $K_{ve}$  is the partition coefficient between the viable epidermis/layer and donor ( $K_{ve} = C_{ve}^{ss}/C_d^{ss}$  at the equilibrium between the viable epidermis/layer and the donor). It is also noted that  $k_p^d$  (eq 2) can be expressed in terms of  $k_p^{sc}$  and  $k_p^{ve}$  by<sup>3-8</sup>  $1/k_p^d = 1/k_p^{sc} + 1/k_p^{ve}$ , where  $k_p^{sc}$  is the stratum corneum permeability coefficient. We have limited this analysis to pseudo-steady-state permeability coefficients  $k_p^{ve}$  and  $k_p^d$  for transport in the viable epidermis and unstirred receptor/donor diffusion layers, as representation of transport by the diffusion equation unnecessarily increases the complexity of the solutions, given that the lag time in the viable epidermis and unstirred diffusion layers is normally very small. While  $Cl_r$  *in vitro* is defined by either sampling rate or flow rate,  $Cl_r$  *in vivo* is defined by the sum of removal by blood flow and clearance by transport into deeper tissues below the application site.<sup>3</sup>

**Laplace Domain Solution**—We now consider the Laplace domain solution of eq 4 with boundary conditions 6–9. The Laplace transform of eq 4 with initial condition 5 is:

$$s \hat{C}_m = D_m \frac{d^2 \hat{C}_m}{dx^2} \quad (10)$$

where hat over function ( $\hat{\phantom{x}}$ ) denotes the Laplace transform.

The Laplace transforms of boundary condition expressions 6–9 are:

$$-D_m \frac{d \hat{C}_m}{dx} \Big|_{x=0} = k_p^d \left( \frac{C_{d0}}{s} - \frac{\hat{C}_m}{K_m} \right) \quad (11)$$

$$-D_m \frac{d \hat{C}_m}{dx} \Big|_{x=h_m} = k_p^{ve} \left( \frac{\hat{C}_r}{K_r} \right) \quad (12)$$

$$V_r s \hat{C}_r = -AD_m \frac{d \hat{C}_m}{dx} \Big|_{x=h_m} - Cl_r \hat{C}_r \quad (13)$$

The general solution to eq 10 is

$$\hat{C}_m(x,s) = A_1 \sinh\left(\sqrt{st_d} \frac{x}{h_m}\right) + B_1 \cosh\left(\sqrt{st_d} \frac{x}{h_m}\right) \quad (14)$$

where  $A_1$  and  $B_1$  are constants independent of  $x$  to be determined by the boundary conditions, and  $t_d$  is the parameter with the dimension of time:

$$t_d = \frac{h_m^2}{D_m} \quad (15)$$

Substitution of  $\hat{C}_m(x,s)$  in the form of eq 14 to boundary condition 11 yields for  $B_1$ :

$$B_1 = \frac{C_{d0}K_m}{s} + \frac{\sqrt{st_d}}{\kappa_d} A_1, \quad (16)$$

where dimensionless parameter  $\kappa_d$  is the relative permeability of the diffusion layer in the donor:

$$\kappa_d = \frac{k_p^d}{k_p^{sc}} \quad (17)$$

and  $k_p^{sc}$  is the permeability coefficient of membrane:

$$k_p^{sc} = \frac{K_m D_m}{h_m} \quad (18)$$

Solving boundary conditions 12 and 13 for  $A_1$  with  $\hat{C}_m(x,s)$  in the form of eq 14 and with  $B_1$  determined in eq 16 yields expression for  $A_1$ :

$$A_1 = -\frac{C_{d0}K_m}{s} \frac{g_2(s)}{g_1(s) + \frac{\sqrt{st_d}}{\kappa_d} g_2(s)} \quad (19)$$

where functions  $g_1(s)$  and  $g_2(s)$  are:

$$g_1(s) = 1 + \frac{\kappa_{ve}}{Cl_{rN} + V_{rN}st_d} + \frac{\kappa_{ve}}{\sqrt{st_d}} \tanh \sqrt{st_d} \quad (20)$$

$$g_2(s) = \left(1 + \frac{\kappa_{ve}}{Cl_{rN} + V_{rN}st_d}\right) \tanh \sqrt{st_d} + \frac{\kappa_{ve}}{\sqrt{st_d}} \quad (21)$$

and dimensionless parameters  $\kappa_{ve}$ ,  $Cl_{rN}$ , and  $V_{rN}$  are defined as:

$$\kappa_{ve} = \frac{k_p^{ve}}{k_p} \quad (22)$$

$$Cl_{rN} = \frac{Cl_r K_r}{k_p^{sc} A} \quad (23)$$

$$V_{rN} = \frac{V_r K_r}{V_m K_m} \quad (24)$$

We note that the kinetic interpretations of parameters introduced here are as follows:  $t_d$  is of the order of magnitude of the diffusion time through membrane;  $\kappa_{ve}$  is a measure of the relative resistance of membrane ( $1/k_p^{sc}$ ) to the resistance of the viable epidermis/aqueous layer ( $1/k_p^{ve}$ );  $Cl_{rN}$  is a measure of the magnitude of the removal rate from the receptor phase ( $Cl_r$ ) relative to transport

through the membrane ( $k_p^{sc}A$ );  $V_{rN}$  is the ratio of the amount of drug in the receptor phase and membrane ( $C_r V_r / [C_m V_m]$ ) assuming equilibrium exists between phases.

Substitution of  $A_1$  from 19 and  $B_1$  from 16 to eq 14 yields the equation for the concentration in the membrane:

$$\hat{C}_m(x,s) = \frac{C_{d0}K_m}{s} \frac{g_1(s) \cosh\left(\sqrt{st_d} \frac{x}{h_m}\right) - g_2(s) \sinh\left(\sqrt{st_d} \frac{x}{h_m}\right)}{g_1(s) + \frac{\sqrt{st_d}}{\kappa_d} g_2(s)} \quad (25)$$

**Flux of Solute**—The flux of solute into the receptor phase is given by:

$$\hat{J}(s) = -D_m \frac{d\hat{C}_m}{dx} \Big|_{x=h_m} \quad (26)$$

Hence, from eqs 25 and 26:

$$\hat{J}(s) = \frac{k_p^{sc} C_{d0}}{s} \left[ \left( \frac{1}{Cl_{rN} + V_{rN}st_d} + \frac{1}{\kappa_{ve}} + \frac{1}{\kappa_d} \right) \cosh \sqrt{st_d} + \left( \frac{1}{\sqrt{st_d}} + \frac{\sqrt{st_d}}{\kappa_d} \left[ \frac{1}{\kappa_{ve}} + \frac{1}{Cl_{rN} + V_{rN}st_d} \right] \right) \sinh \sqrt{st_d} \right]^{-1} \quad (27)$$

**Amount of Solute Absorbed**—The cumulative amount of solute absorbed  $Q(t)$  over time  $t$  into the receptor can be derived from the flux–time relationship for a solute:

$$Q(t) = \int_0^t A J(t') dt' \quad (28)$$

Or in the Laplace domain:

$$\hat{Q}(s) = \frac{A \hat{J}(s)}{s} \quad (29)$$

Hence, from eqs 27 and 29:

$$\hat{Q}(s) = \frac{k_p^{sc} A C_{d0}}{s^2} \left[ \left( \frac{1}{Cl_{rN} + V_{rN}st_d} + \frac{1}{\kappa_{ve}} + \frac{1}{\kappa_d} \right) \cosh \sqrt{st_d} + \left( \frac{1}{\sqrt{st_d}} + \frac{\sqrt{st_d}}{\kappa_d} \left[ \frac{1}{\kappa_{ve}} + \frac{1}{Cl_{rN} + V_{rN}st_d} \right] \right) \sinh \sqrt{st_d} \right]^{-1} \quad (30)$$

**Receptor Phase Concentration**—Combining eqs 26 and 13 yields

$$V_r s \hat{C}_r = A \hat{J}(s) - Cl_r \hat{C}_r \quad (31)$$

Rearrangement yields the receptor concentration  $\hat{C}_r(s)$ :

$$\hat{C}_r(s) = \frac{A \hat{J}(s)}{V_r s + Cl_r} \quad (32)$$

## Simulations and Data Analysis

Simulations in this section have been performed by numerical inversion of functions from the Laplace domain to the time domain using the program SCIENTIST (Micro-Math Scientific software). Numerical inversion of the Laplace domain solutions were used in these simulations for simplicity. The inversion of  $\hat{Q}(s)$  to the time domain for arbitrary  $t$  is only possible in a form of an infinite sum of residues of function  $e^{st} \hat{Q}(s)$  at its singularities and involves solving bulky transcendental equations. A solution in this form

was felt to be of limited value as reliable numerical inversion techniques are now available.<sup>24</sup>

Experimental data illustrating the effect of receptor composition (aqueous solutions containing Volpo N 20 or bovine serum albumin) and sampling times on the penetration of octyl salicylate as a 10% solution in liquid paraffin through 20  $\mu\text{m}$  high density polyethylene membrane were produced by our group.<sup>18,25</sup> In addition, solubilities of octyl salicylate determined in Volpo N 20 6% ( $9.73 \pm 0.21$  mg/mL) and 4% bovine serum albumin ( $0.24 \pm 0.01$  mg/mL)<sup>18,25</sup> were used for data interpretation.

## Results

The present model shows that, under conditions of constant donor concentration, the cumulative amount absorbed  $Q(t)$ , the flux  $J(t)$  and the receptor phase concentration  $C_r(t)$  can be expressed in Laplace domain by eqs 30, 27, and 32, respectively. These values have been expressed in terms of six parameters reflecting both intrinsic and extrinsic determinants of the resulting time profiles. The two usual intrinsic variables are the stratum corneum permeability coefficient ( $k_p^{\text{sc}}$ ) and the diffusion time through the stratum corneum ( $t_d$ ). The extrinsic variables are  $\kappa_d$ ,  $\kappa_{\text{ve}}$ ,  $\text{Cl}_{\text{rN}}$ , and  $V_{\text{rN}}$ . These variables are determined by receptor (dermal) clearance, receptor (dermal) volume (assuming it is effectively well-mixed), receptor phase composition (affinity for solute), viable epidermal (aqueous diffusion layer) resistance, and the vehicle-membrane interfacial resistance. We now consider the effects of each of these determinants on  $Q(t)$ ,  $J(t)$  and  $C_r(t)$  versus  $t$  profiles. Later we express equations 30, 27 and 32 as steady state approximations and consider the explicit effects of each determinant.

**Receptor (Dermal) Clearance**—The effect of receptor (dermal) clearance on  $Q(t)$  versus  $t$  profiles is defined by  $\text{Cl}_{\text{rN}}$ , which expresses  $\text{Cl}_r K_r$  relative to  $k_p^{\text{sc}} A$  (eq 23). Figure 2a shows normalized plots of  $Q/(k_p^{\text{sc}} A C_{\text{d0}} t_d)$  versus  $t/t_d$  for a specific case where both the relative viable epidermis resistance ( $\kappa_{\text{ve}}$ ) and relative receptor volume ( $V_{\text{rN}}$ ) equal 0.5, and there is no donor-stratum corneum interfacial resistance ( $\kappa_d \rightarrow \infty$ ). It is apparent that as  $\text{Cl}_{\text{rN}}$  decreases, corresponding to a reduction in sampling rate, the cumulative amount absorbed decreases in a curvilinear manner. However, at long times, an apparent steady-state flux is reached. Figure 2b shows that decreasing the receptor clearance results in a lower steady-state flux (slope of relationship), a longer time to reach steady state, and, in this case, a negative lag time ( $\text{lag}_2$ ). Figure 2c and Figure 2b show that the flux is reduced and receptor phase concentration increased by decreasing the receptor clearance.

**Receptor (Dermal) Volume**—Figure 3a shows that the volume of the receptor phase, as represented by  $V_{\text{rN}} (= V_r K_r / [V_m K_m])$ , eq 24 also affects the cumulative amount-time profiles. This analysis assumes that this volume is effectively well-mixed. The curvilinear profiles are less pronounced as  $V_{\text{rN}}$  increases. When  $V_{\text{rN}} \rightarrow \infty$ , the profile is equivalent to that for infinite sampling. It is apparent from Figure 3a that reducing the receptor volume results in the same steady-state flux when a finite receptor volume exists, as distinct from the much higher steady-state flux with sink conditions as defined by  $V_{\text{rN}} \rightarrow \infty$ . Figure 3a also shows that decreasing  $V_{\text{rN}}$  decreases the time to reach steady state. Consistent with this observations,  $V_{\text{rN}}$  affects the time for  $C_r(t)$  to reach steady state, but not the actual  $C_{\text{r ss}}$  when a finite volume exists.

**Receptor Solution Composition**—The receptor solution composition will determine the partition coefficient of the solute between the stratum corneum and receptor solution  $K_r$  and, in turn,  $\text{Cl}_{\text{rN}} (= \text{Cl}_r K_r / (k_p^{\text{sc}} A)$ , eq 23) and

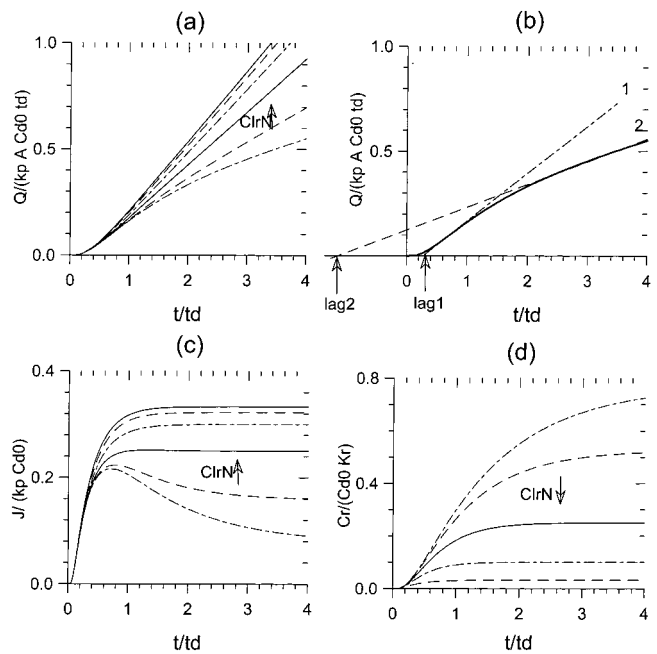


**Figure 2**—(a) Normalized cumulative amount absorbed versus normalized time profiles for  $\kappa_{\text{ve}} = V_{\text{rN}} = 0.5$  and  $\kappa_d = \infty$  based on eq 30 ( $\kappa_{\text{ve}}$  represents ratio of resistance of membrane,  $1/k_p^{\text{sc}}$ , to the resistance of the viable epidermis/aqueous layer,  $1/k_p^{\text{ve}}$ ,  $\kappa_d$  represents ratio of resistance of membrane,  $1/k_p^{\text{sc}}$ , to the resistance of the vehicle-stratum corneum interface,  $1/k_p^{\text{d}}$ , whereas  $V_{\text{rN}}$  defines ratio of receptor-membrane effective distribution volumes). The curves on each graph represent  $\text{Cl}_{\text{rN}}$  values of 0.1, 0.3, 1, 3, 10, and  $\infty$ , with arrows indicating the increase of  $\text{Cl}_{\text{rN}}$  ( $\text{Cl}_{\text{rN}}$  defines relative rate of receptor clearance to permeability through membrane). (b) The curve corresponding to  $\text{Cl}_{\text{rN}} = 0.1$  from part a (solid line) is presented together with its steady-state (dashed line) and quasi-steady-state (dash-dotted line) extrapolations. Intercepts of extrapolations with x axis define negative ( $\text{lag}_2$ ) and positive ( $\text{lag}_1$ ) lag times for the steady and quasi steady states. (c) Normalized flux versus normalized time ( $t/t_d$ ). (d) Normalized receptor concentration versus normalized time.

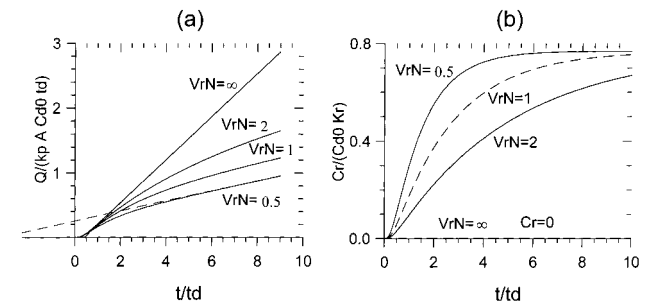


**Figure 3**—(a) Normalized cumulative amount absorbed versus normalized time profiles for different receptor phase volumes (varying  $V_{\text{rN}}$ ) with  $\kappa_{\text{ve}} = 0.5$ ,  $\text{Cl}_{\text{rN}} = 0.1$ , and  $\kappa_d = \infty$ . On each graph, curves represent  $V_{\text{rN}}$  values of 0.5, 1.0, 2.0, and  $\infty$ , respectively, starting from lower curve (see Figure 2 for simplistic description of  $\kappa_{\text{ve}}$ ,  $V_{\text{rN}}$ , and  $\text{Cl}_{\text{rN}}$ ). (b) Corresponding receptor concentrations  $C_r$  normalized for donor concentration  $C_{\text{d0}}$ .

$V_{\text{rN}} (= V_r K_r / (V_m K_m))$ , eq 24). Figure 4a shows that as  $K_r$  decreases, the cumulative amount absorbed also decreases. It is apparent that reduced  $K_r$  is associated with a lower steady-state flux. Given that  $K_r$  is also defined by the solubility in the receptor divided by that in the donor when Henry's law applies, similar profiles can be shown for a given vehicle or donor phase when the receptor composition is characterized by the solubility of the solute in the receptor phase.

Figure 4b shows that a decreased  $K_r$  (and receptor phase solubility for solute) leads to a decreased  $C_r$  but does not greatly affect the time to reach  $C_{\text{r ss}}$ . It is evident in Figure 4c that experimental data, in which the Volpo N20 con-

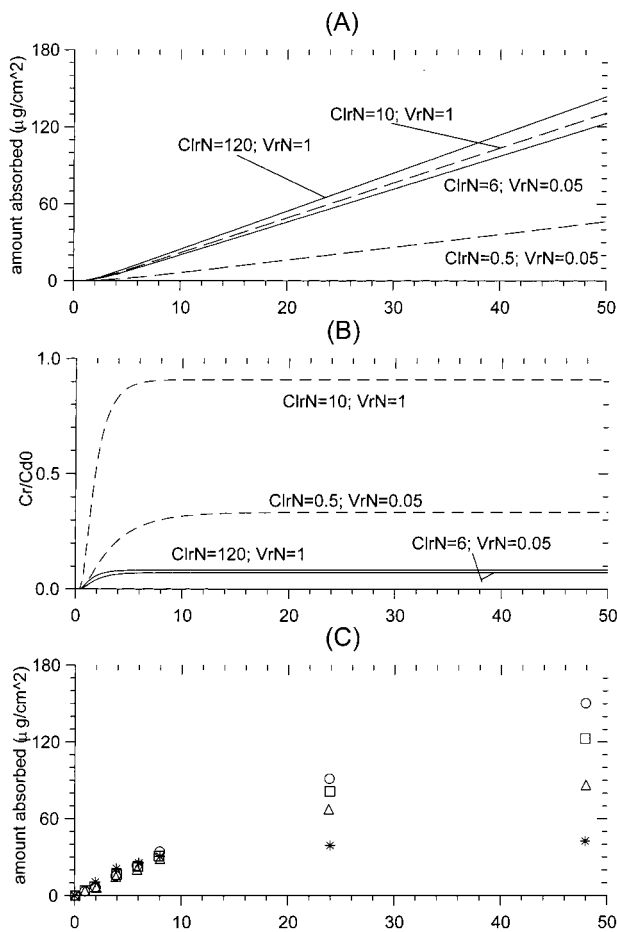


**Figure 4**—Effect of sampling times, sampling rate, and receptor composition on the amount absorbed versus time plots. A: Simulations with eq 48 of a rapid sampling rate (solid lines,  $Cl_{rN} = 12K_r$ , and  $V_{rN} = 0.1K_r$ ) and slower sampling rate (dashed lines,  $Cl_{rN} = K_r$ , and  $V_{rN} = 0.1K_r$ ) for two different partition coefficients  $K_r$  (0.5, 10) and  $t_d = 10$ h; B: corresponding receptor concentration  $C_r$  normalized for donor concentration  $C_{d0}$ ; C: experimental data for 10% octyl salicylate in liquid paraffin (v-v) applied to 20  $\mu$ m high density polyethylene membranes<sup>18,25</sup> with different receptor fluids and a high sampling rate for the first eight hours. (○), (□), (△), and (\*) represent 10% of Volpo-N 20, 6% of Volpo-N 20, 3% of Volpo-N 20, and 4% of bovine serum albumin (BSA) in the receptor phase, respectively.

centration in the receptor phase was reduced, is consistent with lower penetration for receptor phase in which the solute is less soluble. An even lower penetration is observed for the BSA receptor phase in which octyl salicylate is 1/40 the solubility in 6% Volpo N20. Figure 4c also shows that the effects of receptor phase variability on penetration is diminished as the receptor sampling rate is increased.

**Contribution of Viable Epidermis (aqueous diffusion layer)**—Figures 5a and 5b show plots of normalized cumulative amount penetrating versus time when the resistance of the viable epidermis is 1/10th and 10 $\times$ , respectively, that of the stratum corneum. It is apparent that as the relative resistance of the viable epidermis or aqueous diffusion layer increases, the steady-state flux is reduced and the lag time increased. Further, the significant effect of receptor clearance observed when there is a relatively low viable epidermal resistance effectively disappears when the relative resistance is high.

**Contribution of Vehicle–Stratum Corneum Interfacial Resistance**—An effect, similar to that when viable epidermis is significant, applies when the relative resistance of the vehicle–stratum corneum interface is high. Figure 5c and Figure 5d show that when this resistance becomes high, the steady-state flux is reduced, lag time is

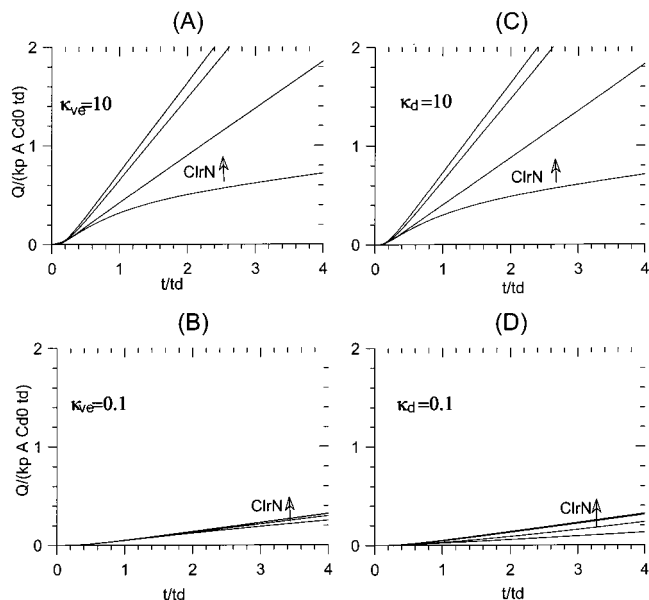


**Figure 5**—(a,b) Effect of epidermal resistance as described by  $\kappa_{ve}$  ( $k_p^{ve}/k_p^{sc}$ ) on normalized amount absorbed versus normalized time profiles for  $V_{rN} = 0.5$  and  $\kappa_d = \infty$ ; (c,d) Effect of vehicle–stratum corneum resistance as described by  $\kappa_d$  ( $k_p^d/k_p^{sc}$ ) on normalized amount absorbed versus normalized time profiles for  $V_{rN} = 0.5$  and  $\kappa_{ve} = \infty$ . The curves on each graph represent  $Cl_{rN}$  values of 0.1, 1, 10, and  $\infty$  starting from the lower curve, respectively.

increased, and removal clearance effects are less pronounced. The receptor (dermal) concentration (not shown) is also decreased.

**Steady-State Approximations**—It is apparent in Figures 2–5 that a steady-state regime is approached at long times ( $t \gg t_d$ ) by  $Q(t)$ ,  $J(t)$ , and  $C_r(t)$ . For ( $t \gg t_d$ ), the resulting  $Q_{ss}(t)$ ,  $J_{ss}$ , and  $C_{r,ss}$  are defined by the singularity at  $s = 0$ . Hence, for  $Q_{ss}(t)$ :

$$Q_{ss}(t) \approx k_p^{sc} A C_{d0} \left( t \lim_{s \rightarrow 0} q(s) + \lim_{s \rightarrow 0} \frac{dq(s)}{ds} \right) \quad (33)$$

where

$$q(s) = \left[ \left( \frac{1}{Cl_{rN} + V_{rN} s t_d} + \frac{1}{\kappa_{ve}} + \frac{1}{\kappa_d} \right) \cosh \sqrt{s t_d} + \left( \frac{1}{\sqrt{s t_d}} + \frac{\sqrt{s t_d}}{\kappa_d} \left[ \frac{1}{\kappa_{ve}} + \frac{1}{Cl_{rN} + V_{rN} s t_d} \right] \right) \sinh \sqrt{s t_d} \right]^{-1} \quad (34)$$

Writing eq 33 in an identical form to that described in equation 1 yields expressions for the steady-state flux,  $J_{ss}$ , and lag time, lag, given by:

$$J_{ss} = C_{d0} k_p^{sc} \left[ 1 + \frac{1}{\kappa_{ve}} + \frac{1}{\kappa_d} + \frac{1}{Cl_{rN}} \right]^{-1} \quad (35)$$

$$\text{lag} = \frac{t_d}{6} \left( 1 + \frac{2(Cl_{rN}^2 \kappa_d + \kappa_{ve} Cl_{rN} \kappa_d + \kappa_{ve} Cl_{rN}^2) + 6(Cl_{rN}^2 + \kappa_{ve} Cl_{rN} - \kappa_{ve} V_{rN} \kappa_d)}{Cl_{rN}(Cl_{rN} \kappa_d + \kappa_{ve} \kappa_d + Cl_{rN} \kappa_{ve} + Cl_{rN} \kappa_{ve} \kappa_d)} \right) \quad (36)$$

The corresponding expression for  $C_{r,ss}$  is

$$C_{r,ss} = \frac{A C_{d0} k_p^{sc}}{Cl_r} \left[ 1 + \frac{1}{\kappa_{ve}} + \frac{1}{\kappa_d} + \frac{1}{Cl_{rN}} \right]^{-1} \quad (37)$$

In the absence of a significant viable epidermis and donor diffusion layer resistance and when sink conditions apply, the steady-state flux due to transport across the stratum corneum  $J_{ss}^{sc}$  is given by  $C_{d0}k_p^{sc}$ . Hence, if the steady-state flux  $J_{ss}$  is defined for given values of  $\kappa_d$ ,  $Cl_{rN}$ , and  $\kappa_{ve}$ ,  $J_{ss}^{sc}$  can be estimated from  $J_{ss}$ ,  $Cl_{rN}$ ,  $\kappa_d$ , and  $\kappa_{ve}$  using eq 35. It is to be noted, that when infinite sink conditions apply,  $Cl_r \rightarrow \infty$  so that  $Cl_{rN} \rightarrow \infty$ , noting  $\kappa_{ve} = k_p^{ve}/k_p^{sc}$ ,  $\kappa_d = k_p^d/k_p^{sc}$  (eqs 22, 17) and  $J_{ss}^{sc} = C_{d0}k_p^{sc}$ , the steady-state flux can be rearranged into the form:

$$J_{ss} = C_{d0} \left( \frac{1}{k_p^{sc}} + \frac{1}{k_p^{ve}} + \frac{1}{k_p^d} \right)^{-1} = C_{d0}k_p \quad (38)$$

where  $k_p$  is the apparent permeability coefficient defined in eq 2 and  $C_{d0}$  is the donor concentration.

The determinants of  $J_{ss}$  under nonsink conditions can be better understood by equating the definition for  $J_{ss}$  defined in eqs 2 and 35:

$$J_{ss} = K_p'(C_{d0} - C_{r,ss}) = C_{d0}k_p^{sc} \left[ 1 + \frac{1}{\kappa_{ve}} + \frac{1}{\kappa_d} + \frac{1}{Cl_{rN}} \right]^{-1} \quad (39)$$

Hence, after some rearrangement

$$K_p' \left( 1 - \frac{C_{r,ss}}{C_{d0}} \right) = \left( \frac{1}{k_p^{sc}} + \frac{1}{k_p^{ve}} + \frac{1}{k_p^d} + \frac{1}{K_p'} \right)^{-1} \quad (40)$$

where  $K_p' (= Cl_r K_p / A)$  is an "effective" removal permeability coefficient for the receptor. Equation 39 could therefore be expressed as:

$$J_{ss} = C_{d0} \left( \frac{1}{k_p^{sc}} + \frac{1}{k_p^{ve}} + \frac{1}{k_p^d} + \frac{1}{K_p'} \right)^{-1} = K_p'' C_{d0} \quad (41)$$

Hence, the "effective" permeability coefficient recognizing nonsink condition  $K_p''$  reflects not only the stratum corneum and viable epidermis permeability coefficients, but also the "effective" removal permeability coefficient and donor interface resistance.

Using eq 32 with  $s = 0$  and  $\hat{J}(0) = J_{ss}$  the steady state concentration in the receptor phase can be defined as:

$$C_{r,ss} = \frac{C_{d0}A}{Cl_r} \left( \frac{1}{k_p^{sc}} + \frac{1}{k_p^{ve}} + \frac{1}{k_p^d} + \frac{1}{K_p'} \right)^{-1} \quad (42)$$

The removal clearance is of particular importance in determining the steady state concentration in the receptor phase  $C_{r,ss}$ . Noting eq 41, eq 42 can be expressed as

$$C_{r,ss} = \frac{C_{d0}AK_p''}{Cl_r} \quad (43)$$

Thus, even if the removal permeability coefficient  $K_p' (= Cl_r K_p / A)$  is not rate limiting in epidermal transport, it may be a significant determinant of local tissue concentrations.

The removal permeability coefficient  $K_p'$  or  $Cl_{rN}$  is also a major determinant of whether lag time is positive or negative. Rearranging eq 36 yields:

$$\text{lag} = \frac{t_d}{6} \left[ 1 + \frac{2 \left( \frac{1}{\kappa_{ve}} + \frac{1}{Cl_{rN}} + \frac{1}{\kappa_d} \right) + 6 \left( \frac{1}{\kappa_{ve}\kappa_d} + \frac{1}{\kappa_d Cl_{rN}} - \frac{V_{rN}}{Cl_{rN}^2} \right)}{\frac{1}{\kappa_{ve}} + \frac{1}{Cl_{rN}} + \frac{1}{\kappa_d} + 1} \right] \quad (44)$$

It is apparent that lag time will approach  $t_d/6$  when  $\kappa_{ve}$ ,  $Cl_{rN}$ , and  $\kappa_d$  are infinitely large. Further, the potential to have a negative lag time, as shown in Figures 2b and 3a will only occur when  $Cl_{rN}$  is small and the receptor volume is relatively large, so that the term in square brackets in eq 44 becomes negative.

In summary the data shown in Figures 2–5 arise from the explicit effects of the vehicle–stratum corneum, stratum corneum, viable epidermal, and "effective" removal permeability constants on  $K_p'$  and, hence,  $J_{ss}$ .  $J_{ss}$  will be largely defined by whichever permeability constant is smallest. The lag time will be determined not only by these variables but also by receptor volume. Finally,  $C_{r,ss}$  is dependent on the relative magnitudes of  $C_{d0}AK_p''$  and  $Cl_r$  (eq 43).

## Discussion

The present work has evolved from our overview of mathematical models in percutaneous absorption<sup>2</sup> and the realization that receptor clearance effects had been only examined to a limited extent. A major impetus for the present study was the apparent inconsistency in the results obtained for the penetration of sunscreens through excised human skin and polyethylene membranes *in vitro*.<sup>18,25,26</sup> It was not until we experimented with different receptor compartments as shown in Figure 4c and confirmed that no receptor depletion had occurred that we became aware of the dominant role of composition and sampling or flow rate on the absorption of the lipophilic solutes. Interestingly, the most commonly used receptor fluid remains pH 7.4 phosphate-buffered saline.<sup>27</sup> It has been suggested that  $C_r(t)$  should not exceed 10% of its saturation solubility,<sup>28</sup> as a consequence a greater variety of receptor phases ranging from 25% (v/v) aqueous ethanol, 50% aqueous methanol, various albumin solutions, and various surfactant solutions<sup>27</sup> may be necessary when the water solubility is less than 10  $\mu\text{g/mL}$ .<sup>29</sup> However, this principle is compromised by effects of solubilizers, particularly on the stratum corneum.<sup>27</sup>

The choice of a suitable receptor solution can also be compromised by a need to maintain skin viability.<sup>19</sup> Macpherson et al.<sup>30</sup> have reported that the pesticide aldrin is absorbed through skin into ethanol–water but not aqueous receptor fluids. However, skin viability was not supported by an ethanol–water system. It may therefore be difficult to find a suitable receptor solution providing both *in vivo* equivalent "sink" conditions and viability. In this instance, it may be preferable to estimate  $K_p'$  from  $Cl_r$  and  $K_r$  and substitute into eq 41 to find  $K_p'$ , i.e.,  $1/K_p' = 1/K_p'' - 1/K_p^r$ . It should be noted that a flow through *in vitro* system will facilitate both skin viability<sup>31</sup> and consistency in  $Cl_r$  over time.

Numerical inversion of Laplace transforms defined by eqs 27 to 32 have been used in this work. The validity of such an approach has been studied by many authors including Purves<sup>32</sup> who showed that numerical inversion of the Laplace transform for the two compartment dispersion model described by Roberts et al.<sup>33</sup> was identical to

the analytical solution given by them. A better understanding of the behavior of a system is often achieved by an examination of the limits of the Laplace solution and the resulting analytical solutions. Such an approach has been described by Guy and Hadgraft<sup>20,22</sup> for other models in percutaneous absorption.

In this work we have reported the steady-state flux and lag time which can be defined from Laplace expressions as  $s \rightarrow 0$ . The resulting expressions show the interrelationship between receptor phase solubility, receptor phase volume, and sampling rate on *in vitro* absorption kinetics, thus allowing an estimation of  $k_p^s$  when  $C_{r\ ss}$  becomes significant. These relationships are also important in quantitatively interpreting the effects of perfusate flow rate on percutaneous absorption<sup>9-11</sup> and the reported underestimated *in vivo* absorption provided by a number of *in vitro* studies on lipophilic solutes.<sup>12-19</sup>

This model is also directly applicable to *in vivo* studies in both humans and animals. The expression given allows the combined effects of epidermal transport kinetics and changing blood flow on *in vivo* absorption to be understood as codeterminants of plasma concentration-time profiles after topical application. This effect is most explicitly apparent in the expressions for the steady-state flux and lag times. Cooper<sup>34</sup> considered some pharmacokinetics of solutes into a single compartmental model after topical application. Similar, but more complex expressions, can be developed when the present model is combined with the disposition of drugs in the body. The *in vivo* pharmacokinetics are probably best described in terms of the Laplace transform of plasma concentration  $\hat{C}_p(s)$ , or another biological concentration effect being expressed as a potentially complex function of parameters describing both the absorption through skin and disposition kinetics in the systemic circulation. As discussed by Roberts *et al.*<sup>2</sup> for a case when plasma concentration does not affect the absorption kinetics (infinite sink condition),  $\hat{C}_p(s)$  can be expressed as a product of the input into the systemic circulation  $\hat{J}(s)$  and disposition in the body  $Cl(s)$  ie  $\hat{C}_p(s) = \hat{J}(s)Cl(s)$ . The solution for  $C_p(t)$  is then most readily obtained by numerical inversion of the resulting Laplace transform  $\hat{C}_p(s)$ . The steady-state plasma concentration in this case is simply  $J_{ss}/CL$ , where  $CL$  is the clearance of solute from the body.

Equation 41 is an extension of expressions given by Scheuplein and Blank<sup>35</sup> and Robinson.<sup>36</sup> Scheuplein and Blank<sup>35</sup> expressed  $k_p^s$  in terms of the skin blood flow in the upper 200  $\mu\text{m}$  of the dermis. They suggested that the removal permeability coefficient was large in comparison to the stratum corneum permeability coefficient, except possibly for small lipid-soluble molecules like octanol and permeant gases. In reality, the removal permeability coefficient *in vivo* is defined by both clearance into perfusing blood and transport into deeper tissues.<sup>37</sup> The latter process, however, normally contributes only 10-30% to the overall removal clearance ( $k_p^s A/K_r$ ). Benowitz *et al.*<sup>38</sup> suggested vasoconstriction of dermal blood vessels by intravenously administered nicotine as a cause for a slowing of nicotine transdermal absorption.

Importantly, eq 43 shows that even if the removal permeability coefficient  $k_p^s (= Cl_r K_r / A)$  is not rate limiting in epidermal transport, it may be a significant determinant of local tissue concentrations. Increased local tissue concentrations have been observed when the local blood flow has been decreased in perfused skin preparations.<sup>39,40</sup> A reduction of effective blood flow by vasoconstriction<sup>41</sup> also leads to higher local tissue concentrations. A reduced form of eq 43 corresponding to the case of  $K_r = 1$ ,  $k_p^{ve}$ , and  $k_p^d$  not being rate limiting has been used to explain structure-permeability absorption relationships.<sup>1</sup>

$$C_{r\ ss} = \frac{C_{d0} A k_p^{sc}}{Cl_r (1 + 1/Cl_{rN})} = \frac{C_{d0} A k_p^{sc}}{Cl_r + k_p^{sc} A / K_r} \quad (45)$$

Roberts<sup>1</sup> has suggested that  $Cl_r \ll k_p^{sc} A / K_r$  for phenols so that their viable epidermal concentrations reflect those applied as aqueous solutions. In contrast, for steroids  $Cl_r \gg k_p^{sc} A / K_r$ , and low concentrations will be found in the viable epidermis. The resulting expression for  $Cl_r \gg k_p^{sc} A / K_r$  is:

$$C_{r\ ss} = \frac{C_{d0} A k_p^{sc}}{Cl_r} \quad (46)$$

Equation 46 is now in the same form as the classical steady-state plasma concentration expression associated with a constant input rate ( $C_{d0} A k_p^{sc}$ ) and clearance from the body.<sup>3</sup>

Removal rate *in vitro* and *in vivo* is a major determinant of the apparent lag time. When  $k_p^{ve}$  and  $k_p^d$  are very large, lag reduces to:

$$\text{lag} = \frac{t_d}{6} \left( 1 + \frac{2Cl_{rN} - 6V_{rN}}{Cl_{rN}(1 + Cl_{rN})} \right) \quad (47)$$

Thus a negative lag is predicted when  $V_{rN} > (Cl_{rN} + 3) Cl_{rN} / 6$ . The remaining complexity of this expression and the difficulty in estimating lag times accurately from experimental data provides some justification in recommending that lag time values be interpreted with caution. In particular, it should be noted that short or negative lag times may be associated with a long time to reach steady state. We therefore consider an approximate estimate of this time when only  $Cl_{rN}$  is rate limiting. When  $\kappa_{ve}, \kappa_d \rightarrow \infty$ , the expression for  $\hat{Q}(s)$  reduces to:<sup>2</sup>

$$\hat{Q}(s) = \frac{k_p^{sc} A C_{d0}}{s^2} \frac{\sqrt{st_d}}{Cl_{rN} + V_{rN} s t_d} \frac{\sqrt{st_d}}{\cosh \sqrt{st_d} + \sinh \sqrt{st_d}} \quad (48)$$

Inverting this equation to time domain yields:

$$Q(t) = Q_{ss}(t) + k_p^{sc} A C_{d0} t_d \sum_{n=1}^{\infty} \frac{\exp(-\gamma_n^2 t_d)}{\gamma_n^4 \frac{d}{dx} f(x)|_{x=-\gamma_n^2}} \quad (49)$$

where  $Q_{ss}(t)$  is defined in eq 1,

$$f(x) = \frac{1}{Cl_{rN} + V_{rN} x} \cosh \sqrt{x} + \frac{\sinh \sqrt{x}}{\sqrt{x}} \quad (50)$$

and  $\gamma_n$  are roots of equation:

$$\tan \gamma = \frac{\gamma}{V_{rN} \gamma^2 - Cl_{rN}} \quad (51)$$

If time to steady state  $t_{ss}$  is defined as the time for  $Q(t) - Q_{ss}(t)$  to become less than  $[Q(0) - Q_{ss}(0)]/e$ , then  $t_{ss}$  can be written as:

$$t_{ss} \approx \frac{t_d}{\gamma_1^2} \quad (52)$$

where  $e$  is the base of the natural logarithm and  $\gamma_1$  is the smallest root of eq 51. When  $(Cl_{rN}/V_{rN})^{1/2} < \pi/2$ , it can be

shown that  $(Cl_{rN}/V_{rN})^{1/2} < \gamma_1 < \pi/2$ , and the upper bound on  $t_{ss}$  is therefore  $t_d V_{rN}/Cl_{rN}$ . Numerical inversion of eq 48 for  $Q(t)$  was used to confirm that  $t_d V_{rN}/Cl_{rN}$  is a reasonable approximation for  $t_{ss}$  for  $Cl_{rN} < 3$  and when lag is negative. Hence, whereas lag is short or negative for large  $V_{rN}$  and small  $Cl_{rN}$ ,  $t_{ss}$  is normally long.

A number of authors have suggested that the viable epidermis or aqueous diffusion layer may be a transport limitation between the stratum corneum and the receptor phase. This limitation could be due to a desorption process<sup>22,42</sup> or a viable epidermis/aqueous diffusion layer resistance.<sup>4,6,7</sup> In each case, an infinitely rapid sampling rate is implicitly assumed. Figure 5 showed that a dominant viable epidermal resistance will reduce the steady-state flux, increase the lag time, and reduce the effect of sampling clearance. A comparison of Figures 5a and 5b shows that the presence of either viable epidermis or equivalent transport limitation or a sampling limitation may be discerned by examining the shapes of the profiles. A viable epidermis transport limitation will be defined by a profile which is similar in shape to the traditional profile in the absence of such a limitation but characterized by a lower steady-state flux. In contrast, a sampling limitation is defined by a curvilinear profile with a negative intercept.

The skin first-pass effect may be important in interpreting some percutaneous absorption studies. Hotchkiss<sup>43</sup> has reviewed the wide range of solutes metabolized by skin. As well as metabolism by skin, there may be an incomplete availability of solutes from vehicles. Skin microflora has been shown to metabolize benzoyl peroxide, glyceryl trinitrate, betamethasone-17-valerate, and estradiol.<sup>43</sup> However, the half-lives for metabolism are often long, limiting the effect on absorption kinetics. In contrast, irreversible adsorption (sometimes with chemical reaction) have been observed with solutes such as hair dyes. Indeed, the competing adsorption provided by hair for hair dyes and other solutes<sup>44</sup> would reduce availability further. In the specific case when there is no epidermal resistance and there is a "perfect" receptor sink, the values for  $J_{ss}$ ,  $Q_{ss}$ , and  $C_{r,ss}$  may be reduced to  $F_m J_{ss}$ ,  $F_m Q_{ss}$ , and  $F_m C_{r,ss}$ <sup>3</sup> where  $F_m < 1$  is the availability of unmetabolized solute due to metabolism in the epidermis. When the epidermal resistance is finite or there is not a "perfect" receptor sink as well as when metabolism or irreversible binding takes place in the stratum corneum, metabolism will affect both the flux profiles and time lags due to the diffusive processes involved. The appropriate model for this situation is developed in a later paper.

The present analysis has also included a vehicle-stratum corneum interfacial permeability constant. Such a term is particularly relevant to transdermal patch systems where a rate-limiting membrane or adhesive may affect or control the rate of delivery from the patch material. The term is also applicable to solutions in which there is an unstirred layer in the vehicle at the interface or when there is a partitioning limitation in the transfer of solute from the vehicle to the stratum corneum. There has been an assumed flux from a constant donor concentration of solute in the vehicle into the stratum corneum in certain of the percutaneous absorption kinetics models.<sup>22</sup> This assumed flux can also be represented by the vehicle-stratum corneum interfacial permeability constant defined in the present model.

The present model has been limited to a constant well-mixed donor vehicle with various permeability "barriers" determining transport. In practice, diffusion in the vehicle may also determine percutaneous absorption. Guy and Hadgraft<sup>45</sup> have recognized such an effect in their evaluation of the effect of applied vehicle thickness on the percutaneous absorption of solutes. When diffusivity in the

vehicle is rate limiting, with permeability "barriers" present, the profiles for  $Q(t)$  versus  $t$  are described by a burst effect.<sup>46</sup> The shapes of the profiles do not differ greatly from those obtained in this work, assuming a constant donor concentration but with accumulation to steady state in the receptor (dermis). Analysis of donor concentrations on the vehicle-stratum corneum interface before or on completion of a percutaneous absorption study or varying the removal rate from the receptor is therefore required to distinguish these two effects.

## Conclusion

This work has shown that the experimental protocol and *in vivo* perfusion conditions can markedly affect percutaneous absorption kinetics. These need to be recognized in undertaking percutaneous absorption studies and their perturbations on the resulting kinetics realized from the shape of the profiles obtained, as discussed in this work. Knowledge of the exact conditions can enable actual permeability coefficients to be estimated from apparent steady-state fluxes. Such calculations are particularly pertinent that nonsink receptor conditions be used to maintain viable skin. A major limitation in assessing the current literature for structure-skin permeability relationships<sup>47,48</sup> is the lack of available experimental information to make the appropriate corrections to reported steady-state permeability constants.

A second outcome of this work is the description of the effects of perfusate flow rate, finite receptor volume, and viable epidermis/aqueous diffusion layer resistance on percutaneous absorption kinetics and dermal concentrations. A necessary limitation in the present work to derive simple Laplace expressions has been the assumption of well-stirred vehicle and receptor phases. A subsequent paper will consider the effects of finite donor volume and epidermal metabolism on percutaneous absorption kinetics.

## References and Notes

1. Roberts, M. S. Structure-permeability considerations in percutaneous absorption. In *Prediction of Percutaneous Penetration*; Scott, R. C., Guy, R. H., Hadgraft, J., Eds., IBC Technical Services: London, 1991; Vol. 2, pp 210-228.
2. Roberts, M. S.; Anissimov, Y. G.; Gonsalvez, R. A. Mathematical models in percutaneous absorption. In *Percutaneous Absorption*, 3rd ed.; Bronaugh, R., Maibach, H. I., Eds., Marcel Dekker: New York, 1998; pp 1-55.
3. Roberts, M. S.; Walters, K. A. The relationship between structure and barrier function of skin. In *Dermal Absorption and Toxicity Assessment*; Roberts, M. S., Walters, K. A., Eds., Marcel Dekker: New York, 1998; pp 1-42.
4. Scheuplein, R. J.; Blank, I. H. Mechanism of percutaneous absorption iv. penetration of non electrolytes (alcohols) from aqueous solutions and from pure liquids. *J. Invest. Dermatol.* **1973**, *60*, 286-296.
5. Roberts, M. S.; Anderson, R. A.; Swarbrick, J. Permeability of human epidermis to phenolic compounds. *J. Pharm. Pharmacol.* **1977**, *29*, 677-683.
6. Roberts, M. S.; Anderson, R. A.; Swarbrick, J.; Moore, D. E. The percutaneous absorption of phenolic compounds: The mechanism of diffusion across the stratum corneum. *J. Pharm. Pharmacol.* **1978**, *30*, 486-490.
7. Cleek, R. L.; Bunge, A. L. A new method for estimating dermal absorption from chemical exposure. 1. General approach. *Pharm. Res.* **1993**, *10*, 497-506.
8. Siddiqui, O.; Roberts, M. S.; Polack, A. E. Percutaneous absorption of steroids relative contributions of epidermal penetration and dermal clearance. *J. Pharmacokinet. Biopharm.* **1989**, *17*, 405-424.
9. Crutcher, W.; Maibach, H. I. The effect of perfusion rate on *in vitro* percutaneous penetration. *J. Invest. Dermatol.* **1969**, *53*, 264-269.
10. Anjo, D. M.; Feldman, R. J.; Maibach, H. I. Methods for predicting percutaneous absorption in man. In *Percutaneous*



- absorption of steroids; Mauvais-Jarvis, P., Vickers, C. F. H., Wepierre, J., Eds., Academic Press: New York, 1980; Chapt. 3.
11. Bronaugh, R. L.; Stewart, R. F. Methods for *in vitro* percutaneous absorption studies IV: The flow-through diffusion cell. *J. Pharm. Sci.* **1985**, *74*, 64–67.
  12. de Lange, J.; van Eck, P.; Bruijnzeel, P. L.; Elliot, G. R. The rate of percutaneous permeation of xylene, measured using the perfused pig ear model, is dependent on the effective protein concentration in the perfusing medium. *Toxicol. Appl. Pharmacol.* **1994**, *127*, 298–305.
  13. Moloney, S. J. The *in vitro* percutaneous absorption of glycerol trioleate through hairless mouse skin. *J. Pharm. Pharmacol.* **1988**, *40*, 819–821.
  14. Roper, C. S.; Howes, D.; Blain, P. G.; Williams, F. M. Prediction of the percutaneous penetration and metabolism of dodecyl decaethoxylate in rats using *in vitro* models. *Arch. Toxicol.* **1995**, *69*, 649–654.
  15. Wester, R. C.; Maibach, H. I.; Bucks, D. A.; McMaster, J.; Mobayen, M.; Sarason, R.; Moore, A. Percutaneous absorption and skin decontamination of PCBs: *in vitro* studies with human skin and *in vivo* studies in the rhesus monkey. *J. Toxicol. Environ. Health.* **1990**, *31*, 235–246.
  16. Roper, C. S.; Howes, D.; Blain, P. G.; Williams, F. M. Percutaneous penetration of 2-phenoxyethanol through rat and human skin. *Food Chem. Toxicol.* **1997**, *35*, 1009–1016.
  17. Kasting, G. B.; Francis, W. R.; Bowman, L. A.; Kinnett, G. O. Percutaneous absorption of vanilloids: *in vivo* and *in vitro* studies. *J. Pharm. Sci.* **1997**, *86*, 142–146.
  18. Jiang, R.; Roberts, M. S.; Prankerd, R. J.; Benson, H. A. E. Percutaneous absorption of sunscreen agents from formulations: self association of octylsalicylate and effects on skin flux. *J. Pharm. Sci.* **1997**, *86*, 791–796.
  19. Bronaugh, R. L. A flow-through diffusion cell. In *In vitro Percutaneous Absorption: Principles, Fundamentals and Applications*; Bronaugh, R. L., Maibach, H. I., Eds., CRC Press: Boca Raton, 1991; pp 17–23.
  20. Guy, R. H.; Hadgraft, J. Theoretical comparison of release rates of drugs into sink and nonsink conditions. *J. Pharm. Sci.* **1981**, *70*, 1243–1245.
  21. Parry, G. E.; Bunge, A. L.; Silcox, G. D.; Pershing, L. K.; Pershing, D. W. Percutaneous absorption of benzoic acid across human skin. *in vitro* experiments and mathematical modelling. *Pharm. Res.* **1990**, *7*, 230–236.
  22. Guy, R. H.; Hadgraft, J. Physicochemical interpretation of the pharmacokinetics of percutaneous absorption. *J. Pharmacokinet. Biopharm.* **1983**, *11*, 189–203.
  23. Bronaugh, R. L.; Stewart, R. F. Methods for *in vitro* percutaneous absorption studies III: Hydrophobic compounds. *J. Pharm. Sci.* **1984**, *73*, 1255–1258.
  24. Yano, Y.; Yamaoka, K.; Tanaka, H. A non-linear least squares program, MULTI(FILT), based on fast inverse laplace transform (FILT) for microcomputers. *Chem. Pharm. Bull.* **1989**, *37*, 1535–1538.
  25. Jiang, R. *Effect of Vehicle Formulation on Skin Permeation of Sunscreen Agents*. Ph.D. dissertation, University of Queensland, 1998.
  26. Jiang, R.; Benson, H. A.; Cross, S. E.; Roberts, M. S. *In vitro* human epidermal and polyethylene membrane penetration and retention of the sunscreen benzophenone-3 from a range of solvents. *Pharm. Res.* **1998**, *15*, 1863–1868.
  27. Brain, K. R.; Walters, K. A.; Watkinson, A. C. Investigation of skin permeation *in vitro*. In *Dermal Absorption and Toxicity Assessment*; Roberts, M. S., Walters, K. A., Eds., Marcel Dekker: New York, 1998; pp 161–187.
  28. Skelly, J. P.; Shah, V. P.; Maibach, H. I.; et al. FDA and AAPS report of the workshop on principles and practices of *in vitro* percutaneous penetration studies: relevance to bioavailability and bioequivalence. *Pharm. Res.* **1987**, *4*, 265–267.
  29. Bronaugh, R. L. *In vitro* methods for the percutaneous absorption of pesticides. In *Dermal Exposure to Pesticide Use*; Honeycutt, R., Zweig, G., Ragsdale, N. N., Eds.; American Chemical Society: Washington, DC, 1985; pp 33–41.
  30. Macpherson, S. E.; Scott, R. C.; Williams, F. M. Percutaneous absorption and metabolism of aldrin by rat skin in diffusion cells. *Arch. Toxicol.* **1991**, *65*, 599–602.
  31. Bronaugh, R. L. Current issues in the *in vitro* measurements of percutaneous absorption. In *Dermal Absorption and Toxicity Assessment*; Roberts, M. S., Walters, K. A., Eds., Marcel Dekker: New York, 1998; pp 155–159.
  32. Purves, R. D. Accuracy of numerical inversion of laplace transforms for pharmacokinetic parameter estimation. *J. Pharm. Sci.* **1995**, *84*, 71–74.
  33. Roberts, M. S.; Donaldson, J. D.; Rowland, M. Models of hepatic elimination: comparison of stochastic models to describe residence time distributions and to predict the influence of drug distribution, enzyme heterogeneity and systemic recycling on hepatic elimination. *J. Pharmacokinet. Biopharm.* **1988**, *16*, 41–83.
  34. Cooper, E. R. Pharmacokinetics of skin penetration. *J. Pharm. Sci.* **1976**, *65*, 1396–1397.
  35. Scheuplein, R. J.; Blank, I. H. Permeability of the skin. *Physiol. Rev.* **1971**, *51*, 702–747.
  36. Robinson, P. J. Prediction-simple risk models and overview of dermal risk. In *Dermal Absorption and Toxicity Assessment*; Roberts, M. S., Walters, K. A., Eds.; Marcel Dekker: New York, 1998; pp 203–229.
  37. Singh, P.; Roberts, M. S. Dermal and underlying tissue pharmacokinetics of salicylic acid after topical application. *J. Pharmacokinet. Biopharm.* **1993**, *21*, 337–373.
  38. Benowitz, N. L.; Jacob, P.; Olsson, P.; Johansson, C. J. Intravenous nicotine retards transdermal absorption of nicotine: evidence of blood flow-limited percutaneous absorption. *Clin. Pharmacol. Ther.* **1992**, *52*, 223–230.
  39. Riviere, J. E.; Sage, B.; Williams, P. L. Y. Effects of vasoactive drugs on transdermal lidocaine iontophoresis. *J. Pharm. Sci.* **1991**, *80*, 615–620.
  40. Cross, S. E.; Roberts, M. S. Importance of dermal blood supply and epidermis on the transdermal iontophoretic delivery of monovalent cations. *J. Pharm. Sci.* **1995**, *84*, 584–592.
  41. Singh, P.; Roberts, M. S. Effects of vasoconstriction on dermal pharmacokinetics and local tissue distribution of compounds. *J. Pharm. Sci.* **1994**, *83*, 783–791.
  42. Kubota, K.; Ishizaki, T. A. Theoretical consideration of percutaneous drug absorption. *J. Pharmacokinet. Biopharm.* **1985**, *13*, 55–72.
  43. Hotchkiss, S. A. M. Dermal metabolism. In *Dermal Absorption and Toxicity Assessment*; Roberts, M. S., Walters, K. A., Eds.; Marcel Dekker: New York, 1998; pp 43–101.
  44. Dressler, W. E. Percutaneous absorption of hair dyes. In *Dermal Absorption and Toxicity Assessment*; Roberts, M. S., Walters, K. A., Eds.; Marcel Dekker: New York, 1998; pp 489–536.
  45. Guy, R. H.; Hadgraft, J. A theoretical description relating skin penetration to the thickness of the applied medicament. *Int. J. Pharm.* **1980**, *6*, 321–332.
  46. Hadgraft, J. Calculations of drug release rates from controlled release devices. The slab. *Int. J. Pharm.* **1979**, *2*, 177–194.
  47. Potts, R. O.; Guy, R. H. Predicting skin permeability. *Pharm. Res.* **1992**, *9*, 663–669.
  48. Roberts, M. S.; Pugh, W. J.; Hadgraft, J.; Watkinson, A. C. Epidermal permeability-penetrant structure relationships: 1. An analysis of methods of predicting penetration of monofunctional solutes from aqueous solutions. *Int. J. Pharm.* **1995**, *126*, 219–233.

## Acknowledgments

We are grateful to the financial support of the National Health & Medical Research Council of Australia and the Queensland and New South Wales Lions Medical Research Foundation.

JS990053I